ATMOSPHERIC SCIENCE LETTERS
Atmos. Sci. Let. **5**: 110–117 (2004)
Published online 8 September 2004 in Wiley InterScience (www.interscience.wiley.com). **DOI:** 10.1002/asl.72

The next generation of NWP: explicit forecasts of convection using the weather research and forecasting (WRF) model

James Done,[1†] Christopher A. Davis[2*†] and Morris Weisman[2‡]
[1] *University of Reading, Department of Meteorology, Reading, UK*
[2] *National Center for Atmospheric Research, Boulder, Colorado, USA*

**Correspondence to:*
Christopher A. Davis, National Center for Atmospheric Research, P.O. Box 3000, Boulder, CO 80307, USA.
E-mail: cdavis@ucar.edu

†*Current Affiliation, National Center for Atmospheric Research, Boulder, Colorado.*

‡*The National Center for Atmospheric Research is sponsored by the National Science Foundation.*

Received: 29 November 2003
Revised: 19 May 2004
Accepted: 24 May 2004

Abstract

The performance of daily convection forecasts from 13 May to 9 July 2003 using the Weather Research and Forecast (WRF) model is investigated. Although forecasts using 10-km grid spacing and parameterized convection are not lacking in prediction of convective rainfall, fully explicit forecasts with a 4-km grid spacing more often predict identifiable mesoscale convective systems (MCSs) that correspond to observed systems in time and space. Furthermore, the explicit forecasts more accurately predict the number of MCSs daily and type of organization (termed *convective system mode*). The explicit treatment of convection in NWP does not necessarily provide a better point specific-forecast, but rather a more accurate depiction of the physics of convective systems. Copyright © 2004 Royal Meteorological Society

Keywords: mesoscale; WRF model; model resolution; mesoscale convective system; forecast verification

1. Introduction

The Bow-Echo and Mesoscale Convective Vortex Experiment (BAMEX)[1] represents two primary objectives related to the study of mesoscale convective systems (MCSs). First was a goal to understand the mechanisms of severe wind production in MCSs, exemplified by severe bow-echoes (Fujita, 1978) and to improve the prediction of such severe weather. Second was a goal to understand the formation of remnant, diabatically produced coherent vortices within MCSs, denoted mesoscale convective vortices (MCVs, Bartels and Maddox, 1991), and further, understand and predict the development of subsequent convection associated with these structures and the feedback of convection onto vortical modes. The overarching strategy was to observe the life cycle of MCSs, through their organization, maturation, dissipation and ultimate downstream regeneration.

Operations were conducted between 20th May and 6th July 2003, from MidAmerica Airport, Illinois, US. The observing domain is shown in Figure 1. Facilities included two P-3 aircraft, each with Doppler radar capability, one dropsonde aircraft and a mobile array of ground-based instruments (Davis *et al*., in press).

The Weather Research and Forecasting (WRF) model (Michalakes *et al*., 2001) was used to provide real-time forecasts to aid observing facility deployment. The model was run at two horizontal grid spacings, 4- and 10-km covering domains shown in Figure 1. These configurations will subsequently be referred to as WRF4 and WRF10, respectively. The model configurations differed mainly in the use of a cumulus parameterization on the 10-km grid, but fully explicit treatment of convection on the 4-km grid. Bryan *et al*. (2003) recommend using grid spacing no greater than 1 km for operational forecasts. However, computational restrictions and the desire for a relatively large domain of integration (Figure 1) precluded grid spacing this small. Weisman *et al*. (1997) demonstrated that a grid spacing of 4 km was adequate to represent the basic structure, mass and momentum transport of idealized MCSs. The present application is believed to be the first extensive test of this result for real cases in a quasi-operational setting. We note that Fowle and Roebber (2003) examined explicit forecasts of convection using the MM5 model, but they used 6-km grid spacing on a much smaller domain. The motivation of the present study is to evaluate the improvement, if any, of numerical forecasts that use an explicit versus a parameterized treatment of MCSs.

[1] See http://www.atd.ucar.edu/dir_off/projects/2003/BAMEX.html for more information about BAMEX.

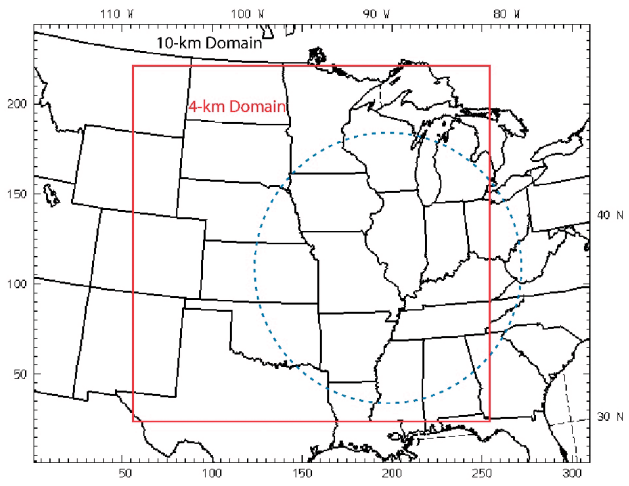

Figure 1. WRF domains; 10-km (black) and 4-km (red–orange) grid spacing. The blue dashed line indicates the nominal BAMEX observing domain

2. Methodology

2.1. Model overview

All domains were initialized from output from the latest available operational Eta model (Black, 1994) run at the National Centers for Environmental Prediction (NCEP). The Eta featured a 12-km grid spacing that was coarsened to 40 km before being obtained from NCEP, and covered much of North America. Both the WRF4 and WRF10 forecasts were initialized at 0000 UTC using the corresponding Eta. Therefore, very little structure was present in the initial conditions on the scale of MCSs (roughly 100–200 km). In general, realistic convective systems and mesoscale structures developed within the first 3 h of the forecast (Skamarock, submitted). Lateral boundary conditions were specified from 3-h output from the corresponding Eta forecast for both WRF forecasts. No nesting of WRF was used.

We used version 1.3 of WRF with 35 vertical levels that were spaced roughly 250 m apart in the lowest kilometer with monotonic stretching to about 1-km spacing near and above 14 km. The model top was at 50 hPa. Both WRF4 and WRF10 used the Yonsei University(YSU) boundary layer scheme (Noh *et al*., 2001), the Oregon State University (OSU) land surface model (Chen and Dudhia, 2001), and the Lin Microphysics scheme (derived from the original scheme described in Lin *et al*., 1983). Microphysical variables (cloud water, cloud ice, rain water, snow and graupel mixing ratios) were initialized to be zero, but appeared to 'spin up' during the first 2 h. While it is desirable to use the same physics schemes for WRF10 and WRF4, we acknowledge that the schemes may perform differently at different grid spacings. An updated version of the Kain–Fritsch convection scheme (Kain, 2004) was included only in WRF10.

2.2. MCS definition and population

The model evaluation follows an object-based approach rather than an approach based on more traditional continuous or categorical verification statistics. Observational datasets include NOWRAD^{TM} radar composite images from Weather Services Inc. as well as soundings and surface data. Daily forecasts are evaluated out to 36 h for both the WRF4 and WRF10.

Houze (1993) defined an MCS as an 'ensemble of thunderstorms' producing a precipitation area extending for at least 100 km in one horizontal direction. In our definition, we require contiguous reflectivity exceeding 35 dBZ over a distance of at least 111 km (1° latitude), with embedded reflectivity of 45 dBZ or greater, and we require that these reflectivity conditions be met for at least 6 consecutive hours.

The simulated reflectivity factor Z was computed from the mixing ratios q_r (rain), q_s (snow) and q_g (graupel) according to $Z = A(\rho q_n)^{1.75}$, where $A = 3.63 \times 10^9$ for rain, 2.19×10^8 for snow and 1.03×10^9 for graupel and ρ is the air density. The reflectivity was then calculated as $10\log_{10}(Z)$. To be consistent with the observed radar composites, the maximum reflectivity in each grid column was used to represent the two-dimensional field examined to identify simulated MCSs.

While many different types of MCSs have been defined in the literature (e.g. Houze, 1993), for simplicity we define only two convective system modes (hereafter simply referred to as modes): non-squall systems and quasi-linear systems. Designation of mode 2 requires a contiguous area at least 111 km long, exceeding 45 dBZ continuously for 6 h. Note that mode 1 systems may briefly satisfy the intensity criteria for mode 2. In Figure 2 are shown examples of forecast and observed systems of each mode. The system depicted in (a) and (b) was an intense squall line that lasted more than 24 h in both the WRF4 forecast and in the observations. The system depicted in (c) and (d) was triggered and organized within the circulation of an MCV.

Convective areas were considered to be distinct systems if they attained the above criteria for 6 h and remained separated from other areas by at least 111 km (distance measured by the separation of 35-dBZ reflectivity regions). In the event of system merger or separation, both systems had to be isolated for at least 6 h in order for the two systems to be recorded. Otherwise, assuming that at least one of the two systems satisfied the intensity and duration criteria outlined above, only a single system was recorded.

The position of a system at any time was estimated from the approximate centroid of reflectivity exceeding 35 dBZ (mode 1), or 45 dBZ (mode 2). In the quasi-linear MCSs, this position was typically the geometric center of the convective line or the apex of a curved line.

Because the WRF10 forecasts use both explicit and implicit precipitation schemes, one could not use

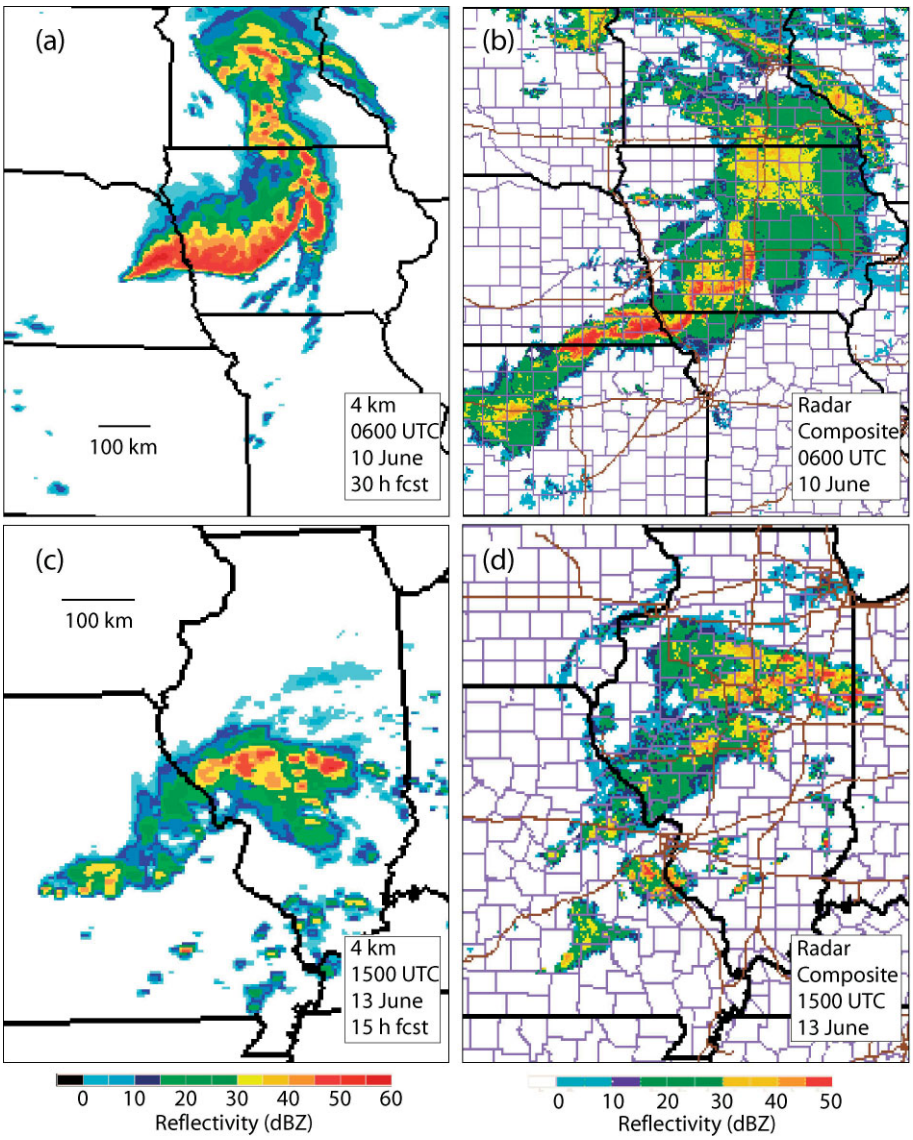

Figure 2. Examples of predicted (from WRF4) and observed MCSs of different types, quasi-linear systems (a) and (b) (system mode 2), and non-squall systems (c) and (d) (system mode 1). Times shown are; (a) and (b), 0600 UTC 10 June, 2003; (c) and (d), 1500 UTC 13 June, 2003. Shown in (a) and (c) is model-derived maximum reflectivity in each grid column (dBZ) and in (b) and (d) appear observed maximum reflectivity in each column (2-km grid)

reflectivity to define the presence of an MCS in WRF10 forecasts. Only 3-h precipitation data were archived from WRF10 forecasts, hence we were forced to identify MCSs on the basis of 3-h accumulations. We defined an MCS in the WRF10 forecasts as a contiguous area of three-hourly rainfall greater than 12.8 mm (roughly 0.5 inches), at least 111 km in length occurring for each of three successive time periods. This ensured that identified systems lasted for at least 6 h. Given a typical Z-R relationship between rainfall and reflectivity of $Z = 300R^{1.4}$, with R in mm h^{-1}, this rainfall threshold corresponds to about 33 dBZ, nearly the threshold reflectivity used to identify systems in the WRF4 forecasts and observations. In Figure 3 are shown three-hourly rainfall from both WRF4 and WRF10 forecasts valid at the times shown in Figure 2. The position of an MCS in the WRF10 forecast was the centroid of the precipitation region exceeding 12.8 mm in 3 h.

There were fundamental difficulties in deriving the convective system mode from the WRF10 forecasts. Therein, convective systems were represented both by so-called grid-resolved and parameterized convection. This made it impossible to draw direct comparisons with radar signatures to define the convective system mode. While a detailed examination of the more complete WRF10 output might reveal some means of discerning the system mode, these characteristics were not readily apparent in fields such as rainfall. Furthermore, in many cases we were not even able to identify precipitation features as an MCS, much less extract information about convective system mode. Hence, we only will consider the system mode identified in the WRF4 forecasts in the remainder of this article.

Although both WRF forecasts extended for 36 h, we only included systems whose midpoint in time (average of beginning and ending times) occurred between 10 UTC (10-h forecast) and 9 UTC the following

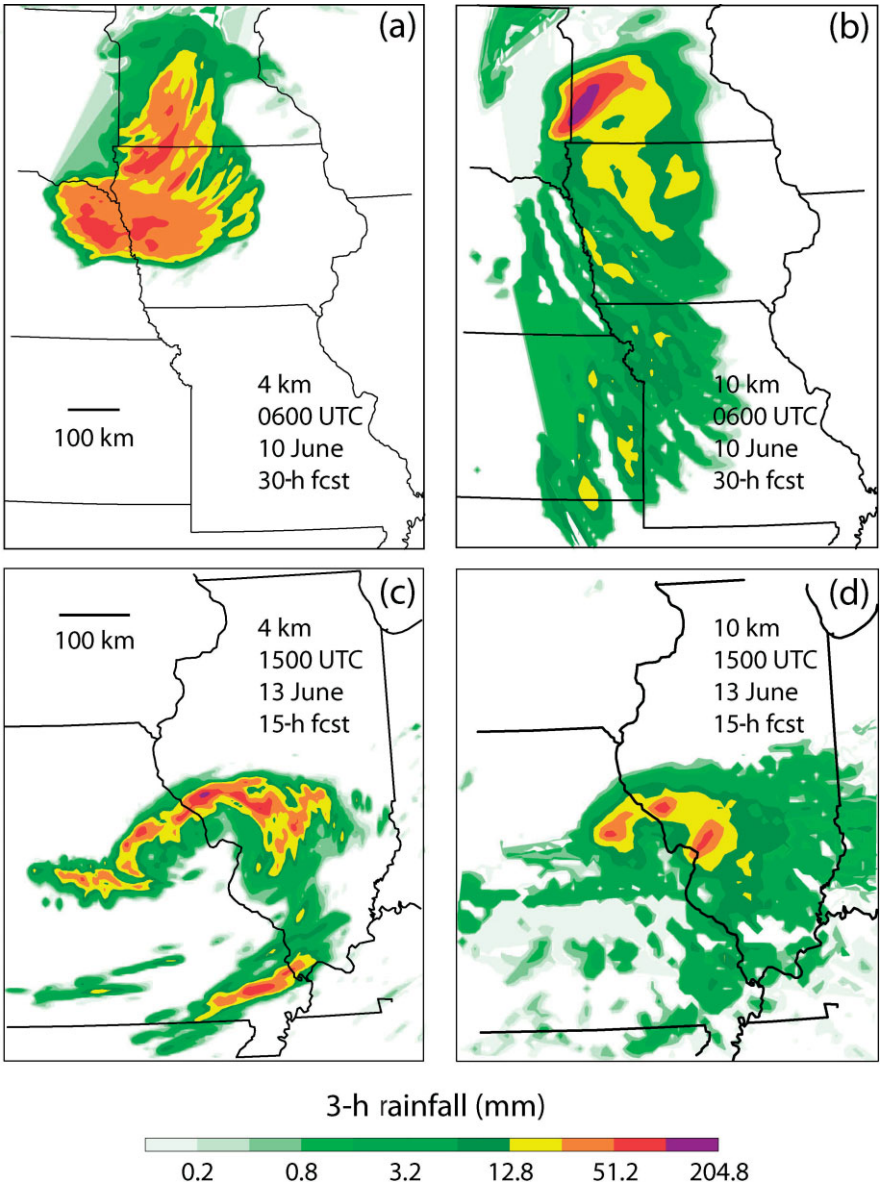

Figure 3. 3-h rainfall from WRF4 and WRF10 forecasts corresponding to times in Figure 2

night (33-h forecast). This restriction reduced the effects of model spin up on MCS prediction. We also ensured that there were no inclusions of 'matching' MCSs occurring in successive forecasts. Because there was a 12-h overlap of successive forecasts (the period 0000–1200 UTC), it was possible for very similar MCSs to appear in successive forecasts. By removing such redundancy, forecasts could be considered independent.

3. Results

3.1. Population

There were a total of 142 observed convective systems satisfying the criteria outlined above between 13 May and 9 July. We recorded 109 MCSs in the WRF4 forecasts, and 99 in the WRF10 forecasts. Roughly 60% of the observed MCSs were classified as mode 2, compared to 54% for the WRF4 forecasts.

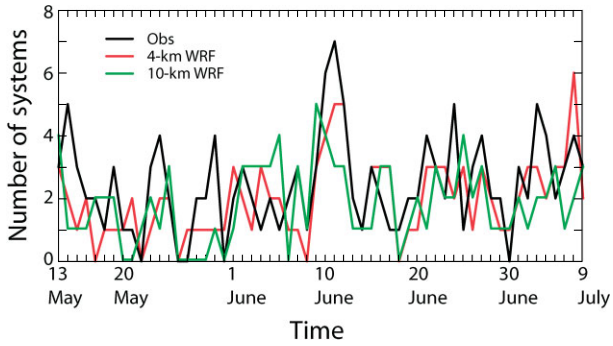

Figure 4. Time series of number of MCSs (without regard to mode) for each forecast. The black line represents observed MCSs, the red line represents MCSs from WRF4 and the green line represents WRF10

Examining the period from 13 May to 9 July on a daily basis, we found that the daily variation in

the number of MCSs in the WRF4 forecasts tracked the daily variation of observed MCSs fairly well (Figure 4). The daily variation of MCSs in the WRF10 forecasts also shows some correlation with the number of observed systems, but to a lesser extent. Computing the anomaly correlation of each time series of forecasts with the observed time series, we find a correlation of 0.57 for the WRF4 forecasts and 0.35 for the WRF10 forecasts. Here, we have computed anomalies as the deviation of the daily number of MCSs from the average of the respective time series. These averages, expressed as MCSs per day, are 2.5, 2.0 and 1.8 for the observations, WRF4 and WRF10, respectively.

3.2. Correspondence

A central question is whether objects (MCSs) in the observational and model datasets correspond. Correspondence is a looser criterion than point-specific accuracy. It merely identifies forecast objects that have a unique observational counterpart that may be displaced in space or time from its forecast location. Such correspondence is routinely considered for forecasts of large-scale weather systems (e.g. cyclones, fronts) and mesoscale weather systems such as hurricanes. Herein, corresponding systems were identified if their predicted and observed time and location differed by no more than 3 h and a spatial distance E (expressed in degrees of latitude) at the beginning, middle *or* ending time. The beginning of an MCS was the first time and location at which the MCS threshold was exceeded (at least mode 1 organization), and the ending was the time and location of the last time that a system exceeded the minimal MCS requirements. The middle time is the average of beginning and ending times. Correspondence was independent of convective system mode.

To help summarize results, it is convenient to introduce the standard 2×2 contingency table for dichotomous events (Wilks, 1995). In Table 1, the four entries are: (a) hits (correct forecasts of event occurring); (b) misses (event observed but not predicted); (c) false alarms (event predicted but not observed); and (d) correct negatives (correct forecasts of event not occurring). Some commonly used statistics are the probability of detection, $\mathrm{POD} = \mathrm{a}/(\mathrm{a}+\mathrm{b})$; false alarm rate, $\mathrm{FAR} = \mathrm{c}/(\mathrm{a}+\mathrm{c})$, the critical success index, $\mathrm{CSI} = \mathrm{a}/(\mathrm{a}+\mathrm{b}+\mathrm{c})$, and the equitable threat score, $\mathrm{ETS} = \mathrm{a}-\mathrm{e}/(\mathrm{a}-\mathrm{e}+\mathrm{b}+\mathrm{c})$, where $\mathrm{e} = (\mathrm{a}+\mathrm{b})(\mathrm{a}+\mathrm{c})/(\mathrm{a}+\mathrm{b}+\mathrm{c}+\mathrm{d})$ is an estimate of the number of hits from a random forecast.

Table 1. Template for standard 2×2 contingency table (Wilks, 1995)

		Observations	
Contingency table		**Yes**	**No**
Forecasts	Yes	(a) Hits	(c) False alarms
	No	(b) Misses	(d) Correct negatives

Table 2. Middle column: number of corresponding systems as a function of minimum position error (E); red for WRF4, blue for WRF10. Right column: critical success indices as a function of E

Min. position error (E)	# Corresponding (4 km/10 km)	CSI (4 km/10 km)
$E < 1°$	26/15	0.13/0.08
$E < 2°$	50/25	0.27/0.13
$E < 3°$	58/42	0.30/0.21
$E < 4°$	63/51	0.33/0.26

Table 2 summarizes the correspondence statistics for both WRF4 and WRF10 forecasts. The CSI values were 0.30 for the WRF4 forecasts and 0.21 for the WRF10 forecasts when we required $E < 3°$ (333 km). The variation of CSI using different distance thresholds reveals that correspondence occurred systematically more often in the WRF4 forecasts, especially for $E < 2°$ (222 km).

3.3. Prediction of convective system mode

As suggested in Section 3a, WRF4 can represent convective system modes similar to those observed. Here we ask how predictable is the convective system mode, both for individual MCSs and within individual forecasts (i.e. the 'mode of the day'). Considering the 63 corresponding MCSs, WRF4 correctly identified the mode 71% of the time. By comparison, unbiased random guessing would yield a 45% success rate.

We now consider the standard contingency table for dichotomous forecasts (Table 3) such that mode 2 is identified with a 'yes' forecast or observation. We obtained a POD of 0.80, a FAR of 0.23, and a CSI of 0.65. An unbiased random forecast produces a POD of 0.67 and a FAR of 0.33. These results demonstrate that WRF4 had skill in predicting the convective system mode on a case-by-case basis. It was also true that statistics of system mode prediction were relatively insensitive to the criteria used to define correspondence.

If we consider the 'mode of the day', that is, predicting whether an MCS with a quasi-linear convective system will occur or not (again, a binary decision), WRF4 was correct on 43 out of 58 days (74%) (Table 4). As can be derived from the contingency table (Table 4) the POD was 0.75 and the FAR was 0.11. Viewed another way, if the WRF4 predicted a

Table 3. Contingency table for dichotomous forecasts of convective system mode, where a 'yes' implies a predicted or observed mode of 2, that is, a quasi-linear MCS

		Observations	
Mode for corresponding convective systems		**Yes (*mode* = 2)**	**No**
Forecasts	Yes (mode = 2)	(a) Hits = 33	(c) False alarms = 10
	No	(b) Misses = 8	(d) Correct negatives = 12

Table 4. Contingency table for system mode 2 for each forecast period, 58 total, where an event is the prediction or observation of system mode 2, and a nonevent is the forecast or observation of no MCS or system mode 1

Most organized mode for each forecast period		Observations	
		Yes (*mode* = 2)	**No**
Forecasts	Yes (mode = 2)	(a) Hits = 33	(c) False alarms = 4
	No	(b) Misses = 11	(d) Correct negatives = 10

quasi-linear MCS, there was an 89% chance that one would be observed. From the standpoint of BAMEX planning, this was extremely useful information for assessing the likelihood of operations during the subsequent afternoon or night.

3.4. Equitable threat scores

The ETS and bias scores have been traditionally used to verify rainfall forecasts (e.g. Olson *et al*., 1995), and it is natural to inquire how the WRF4 and WRF10 forecasts performed against these metrics. Here, we coarsened the observations and WRF4 forecasts to a 10-km grid by area-averaging the fields. From Figure 5, it is apparent that the WRF10 forecasts exhibited a greater total 24-h rainfall (accumulated from 12–36 h during the forecast) than WRF4 with a greater systematic bias. However, the ETS for the WRF10 forecasts was slightly greater than for the WRF4 forecasts. This result appears at odds with the superior performance of the WRF4 from an object-based perspective and reinforces the idea that verification of convection forecasts using the ETS metric can yield an incomplete interpretation of model behavior, consistent with results of Kain *et al*. (2003).

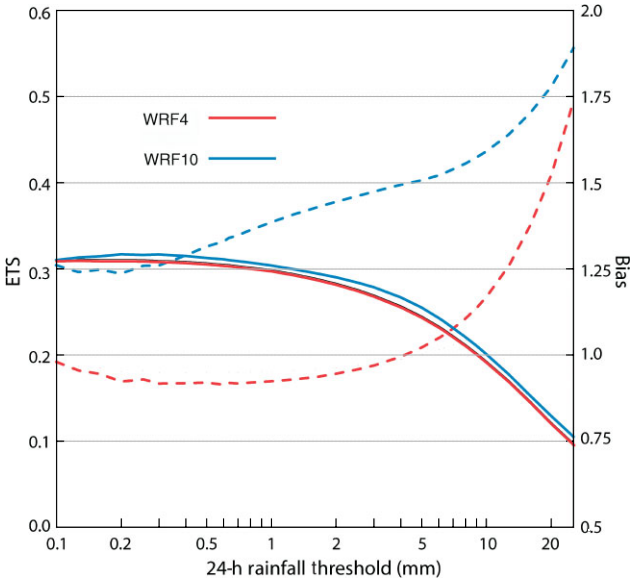

Figure 5. Equitable threat score (solid) and bias (dashed) for WRF4 (red–orange) and WRF10 (blue) forecasts respectively, as a function of 24-h rainfall accumulation (mm). The domain of verification was 32°–46°N, 105°–85°W and the forecast period was 12 to 36 h

The utility of the forecast is another matter. It may very well turn out that the forecast with a higher ETS is more useful, even if it cannot identify the dynamical structure producing the rain. *What we have shown is that the benefit of moving to explicit treatment of convection is not necessarily a better point-specific forecast, but rather a more accurate depiction of the physics of convective systems*. This result may have just as much relevance to climate or regional climate simulations (computing power limitations aside) as it does to weather forecasting.

3.5. Other attributes of corresponding systems

Herein we will discuss position, propagation and duration errors for corresponding objects with $E < 4°$ (bottom row of Table 2). Table 5 shows mean position errors (forecast-observations) at the beginning and ending times for the corresponding MCSs in the WRF4 and WRF10 forecasts. To a good approximation, 'x' and 'y' are synonymous with the east–west and north–south directions respectively. The WRF4 forecasts exhibited a significant northward bias at the beginning of the MCS lifecycle, and an eastward and southward bias at the end. The sign reversal in meridional bias was highly significant and indicated the tendency of forecast systems to propagate to the right (southward) of their observed counterparts. The mean error in the propagation direction was about 23° to the right of the observed path. It turned out that the mean phase speed of forecast MCSs was slightly slower than observed, 17.3 m s^{-1} versus 19.7 m s^{-1}. Therefore, the eastward bias at the end of the MCS lifecycle was due to an excessive duration of forecast systems.

Forecast MCSs on the 10-km grid revealed a bias to the north and east at the ending time, consistent with a slight movement bias to the left of the observed MCS. Since MCS location was based on the centroid of heavy precipitation, this northward and eastward bias may have resulted from heavier total precipitation occurring where explicit precipitation rates were significant. The mean speed of the observed MCSs in this sample was only 16.3 m s^{-1} and the mean speed of the WRF10 MCSs was only 12.9 m s^{-1}. In spite of this speed bias, WRF10 MCSs had greater durations than their corresponding observed systems and this resulted in an eastward bias at the ending time. Collectively, the WRF10 MCSs corresponded to

Table 5. Position errors (forecast minus observation) for 'x' (east–west) and 'y' (north–south) directions expressed in km. Red text indicates values statistically significant at greater than 99% confidence

	$\Delta x_{initial}$	Δx_{final}	$\Delta y_{initial}$	Δy_{final}
WRF4	50	170	94	−78
WRF10	11	125	56	129

a more slow moving population of observed systems than did the WRF4 forecasts. Coupled with a greater negative speed bias for WRF10 MCSs, this resulted in a dramatic difference between speeds of WRF4 and WRF10 MCSs that corresponded to observations (17.3 and 12.9 m s^{-1} respectively). It is likely, however, that the propagation characteristics of WRF10 MCSs will depend strongly on the details of the convection scheme (e.g. Raymond, 1987; Kain *et al*., 2001).

It has been demonstrated from numerical simulations that MCSs with strong attendant cold pools move to the right of the mean flow and vertical wind shear in the lower troposphere in the presence of earth's rotation (Skamarock *et al*., 1994). This propagative effect increases with cold pool amplitude. Thus, it is tempting to conclude that cold pools in the WRF4 MCSs were much stronger than in the WRF10 MCSs. A preliminary analysis suggests this may have been the case, but a more extensive verification effort, to appear in a future article, is needed to quantify the source(s) of the propagation differences.

4. Conclusions

In support of the observations collection during BAMEX, the WRF model provided 36-h forecasts on grids of 4 and 10 km (denoted WRF4 and WRF10 respectively). Because the 4-km grid did not use a cumulus parameterization, comparison of these forecasts gave insight into the benefits of explicitly treating convection in NWP models. This paper has conducted an object-based verification of the prediction of MCSs over central North America during the period 13 May to 9 July 2003, with an emphasis on errors of location, timing and the system mode of convection.

Criteria for MCS identification in WRF10 and WRF4 were based on observed MCSs. The inability of WRF10 to reproduce such characteristics in many cases made it difficult to identify precipitation features as MCSs. Furthermore, the precipitation fields in cases for which an MCS was identified often failed to show system structure, therefore handicapping skill scores, correspondence statistics and characterization of convective system mode. WRF4 forecasts were superior to WRF10 forecasts in terms of the percentage of systems that corresponded to an observed MCS, and in their ability to identify the number of MCSs that would occur each day. The critical success index for MCS correspondence was roughly 1.5 times larger for the WRF4 forecasts compared to that for WRF10. Furthermore, the explicit treatment of convection (that is, avoidance of a cumulus parameterization) allowed a more accurate depiction of the physics of convective systems and a relatively straightforward identification of the convective system mode in the WRF4 forecasts. Prediction of whether an MCS would take the form of a quasi-linear system or less organized convection was correct in more than 70% of forecast MCSs with an observed counterpart. There was some evidence that the WRF4 was capable of finer distinctions of convective system attributes such as the presence of MCVs, bow-echoes or lines of supercell storms, but such distinctions had less robust statistics and were not discussed herein. System mode identification in the WRF10 forecasts was problematic because there were no obvious signals of system structure in the precipitation fields.

The position and propagation of forecast MCSs corresponding to observed systems was also evaluated. Systems in the WRF4 forecasts initiated too far north, propagated more toward the south than observed and lasted too long, resulting in an eastward and southward bias of the forecast MCS termination location. Systems in the WRF10 forecasts moved to the north of the observed MCSs, resulting in a significant positive meridional position error. Forecast MCSs in WRF10 moved more than 4 m s^{-1} more slowly than WRF4 MCSs. We noted numerous instances of excessive rainfall within the convective line of MCSs in WRF4 and the lack of an adequate stratiform region, although these attributes were not evaluated statistically. A more detailed evaluation of rainfall and surface parameters (density, wind, etc.) is planned, and will perhaps discern the cause of the propagation errors in these forecasts.

Acknowledgements

Dr James Done was supported by the Rupert Ford Travel Award administered by the Royal Meteorological Society. The authors are indebted to many National Center for Atmospheric Research (NCAR) personnel for performing the WRF simulations. These include Wei Wang, James Bresch and Jordan Powers of the Mesoscale and Microscale Division and Jeff Keuhn, George Fuentes, Marc Genty and numerous other staff of NCAR's Scientific Computing Division. The authors also wish to thank Dr Jack Kain and an anonymous reviewer for their helpful comments.

References

Bartels DL, Maddox RA. 1991. Midlevel cyclonic vortices generated by mesoscale convective systems. *Monthly Weather Review* **119**: 104–118.

Black TL. 1994. The new NMC mesoscale Eta model: description and forecast examples. *Weather Forecasting* **9**: 265–278.

Bryan GH, Wyngaard JC, Fritsch JM. 2003. Resolution requirements for the simulation of deep moist convection. *Monthly Weather Review* **131**: 2394–2416.

Chen F, Dudhia J. 2001. Coupling an advanced land surface–hydrology model with the Penn State–NCAR MM5 modeling system. Part I: model implementation and sensitivity. *Monthly Weather Review* **129**: 569–585.

Davis C, Atkins N, Bartels D, Bosart L, Coniglio M, Bryan G, Cotton W, Dowell D, Jewett B, Johns R, Jorgensen D, Knievel J, Knupp K, Lee W-C, McFarquhar G, Moore J, Przybylinski R, Rauber R, Smull B, Trapp J, Trier S, Wakimoto R, Weisman M, Ziegler C. In press. The Bow-Echo and MCV Experiment (BAMEX): observations and opportunities. *Bulletin of the American Meteorological Society*.

Fowle MA, Roebber PJ. 2003. Short-range (0–48 h) numerical prediction of convective occurrence, mode and location. *Weather Forecasting* **18**: 782–794.

Fujita TT. 1978. Manual of downburst identification for project NIMROD. Satellite and Mesometeorology Research Paper No. 156, Department of Geophysical Sciences, University of Chicago, 104.

Houze RA. 1993. *Cloud Dynamics*. Academic Press: San Diego; 573.

Kain JS. 2004. The Kain–Fritsch convective parameterization: an update. *Journal of the Applied Meteorology* **43**: 170–181.

Kain JS, Baldwin ME, Janish PR, Weiss SJ. 2001. Utilizing the Eta model with two different convective parameterizations to predict convective initiation and evolution at the SPC. Preprints, Ninth Conference on Mesoscale Processes. Ft. Lauderdale, FL, 91–95.

Kain JS, Baldwin ME, Janish PR, Weiss SJ, Kay MP, Carbin G. 2003. Subjective verification of numerical models as a component of a broader interaction between research and operations. *Weather Forecasting* **18**: 847–860.

Lin Y-L, Farley RD, Orville HD. 1983. Bulk parameterization of the snow field in a cloud model. *Journal of Climate and Applied Meteorology* **22**: 1065–1092.

Michalakes J, Chen S, Dudhia J, Hart L, Klemp J, Middlecoff J, Skamarock W. 2001. Development of a next generation regional weather research and forecast model. In *Developments in Teracomputing: Proceedings of the Ninth ECMWF Workshop on the Use of High Performance Computing in Meteorology*, Zwieflhofer W, Kreitz N(eds). World Scientific: Singapore; 269–276.

Noh Y, Cheon WG, Raasch S. 2001. The improvement of the K-profile model for the PBL using LES. In *Preprints of the International Workshop of Next Generation NWP Model*. Laboratory for Atmospheric Modeling Research: Seoul, South Korea; 65–66.

Olson DA, Junker NW, Korty B. 1995. Evaluation of 33 years of auantitative precipitation forecasting at the NMC. *Weather Forecasting* **10**: 498–511.

Raymond DJ. 1987. A forced gravity wave model of self-organizing convection. *Journal of the Atmospheric Sciences* **44**: 3528–3543.

Skamarock WC. Submitted. Evaluating mesoscale NWP models using kinetic energy spectra. *Monthly Weather Review*.

Skamarock WC, Weisman ML, Klemp JB. 1994. Three-Dimensional evolution of simulated Long-Lived squall lines. *Journal of the Atmospheric Sciences* **51**: 2563–2584.

Weisman ML, Skamarock WC, Klemp JB. 1997. The resolution dependence of explicitly modeled convective systems. *Monthly Weather Review* **125**: 527–548.

Wilks DS. 1995. *Statistical Methods in Atmospheric Sciences: An Introduction*. Academic Press: 467: 238–242.

